

ADIPOSE STEM CELL TREATMENT IN MICE ATTENUATES LUNG AND SYSTEMIC INJURY INDUCED BY CIGARETTE SMOKING

Kelly Schweitzer^{1,2}, Brian H. Johnstone^{3,4}, Jana Garrison^{1,2}, Natalia Rush^{1,2}, Scott Cooper⁵, Dmitry O. Traktuev^{3,4}, Dongni Feng^{3,4}, Jeremy J. Adamowicz^{1,2}, Mary Van Demark^{1,2}, Amanda J. Fisher^{2,6}, Krzysztof Kamocki^{2,7}, Mary Beth Brown^{1,2}, Robert G. Presson, Jr.^{2,6}, Hal E. Broxmeyer^{4,5}, Keith L. March^{3,4,8*}, and Irina Petrache^{1,2,4,8*}

From the ¹ Division of Pulmonary and Critical Care Medicine; ²Center for Immunobiology; ³Division of Cardiology; ⁴Indiana Center for Vascular Biology and Medicine and VC-CAST Signature Center; ⁵Department of Microbiology and Immunology; ⁶Department of Anesthesiology; ⁷Department of Biochemistry and Molecular Biology; ⁸Roudebush Veteran Affairs Medical Center, Indiana University, Indianapolis, IN.

Request reprints from: Irina Petrache, MD, Indiana University, Division of Pulmonary, Allergy, Critical Care and Occupational Medicine, Walther Hall-R3 C400, 980 W. Walnut Street, Indianapolis, IN 46202-5120. Phone: 317-988-3811, Fax 317-988-3976, Email: ipetrach@iupui.edu

***Address correspondence to:** Irina Petrache, MD, Indiana University, Division of Pulmonary, Allergy, Critical Care and Occupational Medicine, Walther Hall-R3 C400, 980 W. Walnut Street, Indianapolis, IN 46202-5120. Phone: 317-988-3811, Fax 317-988-3976, Email: ipetrach@iupui.edu **and to:** Keith March, MD, PhD, IB441, 975 W. Walnut St, Indianapolis, IN 46202. Phone 317-278-0130, Fax 317-278-0089, Email: kmarch@iupui.edu

Sources of support: IUPUI Signature Center for Vascular and Cardiac Adult Stem Cell Therapy; and Krannert Institute; (KM, IP); NIH-NHLBI: Contract grant numbers: R01 HL 077328 (IP) and R01 HL090950 (IP); R01 HL077688 (KLM), T32 HL077688 (DOT), T32 HL091816 (MBB); VA Merit Review Award (KLM); and the Cryptic Mason's Medical Research Foundation

"This article has an online data supplement, which is accessible from this issue's table of content online at www.atsjournals.org"

Running head: ASC ameliorate emphysema

ABSTRACT

Rationale: Adipose-derived stem cells express multiple growth factors that inhibit endothelial cell apoptosis, and demonstrate substantial pulmonary trapping following intravascular delivery.

Objectives: We hypothesized that adipose stem cells would ameliorate chronic lung injury associated with endothelial cell apoptosis, such as that occurring in emphysema.

Methods: Therapeutic effects of systemically-delivered human or mouse adult adipose stem cells were evaluated in murine models of emphysema induced by chronic exposure to cigarette smoke or by inhibition of vascular endothelial growth factor receptors.

Measurements and Main Results: Adipose stem cells were detectable in the parenchyma and large airways of lungs up to 21 days following injection. Adipose stem cell treatment was associated with reduced inflammatory infiltration in response to cigarette smoke exposure, as well as markedly decreased lung cell death and airspace enlargement in both models of emphysema. Remarkably, therapeutic results of adipose stem cells extended beyond lung protection by rescuing the suppressive effects of cigarette smoke on bone marrow hematopoietic progenitor cell function, and by restoring weight loss sustained by mice during cigarette smoke exposure. Pulmonary vascular protective effects of adipose stem cells were recapitulated by application of cell-free conditioned medium, which improved lung endothelial cell repair and recovery in a wound injury repair model and antagonized effects of cigarette smoke *in vitro*.

Conclusions: These results suggest a useful therapeutic effect of adipose stem cells on both lung and systemic injury induced by cigarette smoke, and implicate a lung vascular protective function of adipose stem cell-derived paracrine factors.

Keywords: Pulmonary Disease, Chronic Obstructive; endothelium; cell death; regenerative medicine; human; mouse.

INTRODUCTION

Chronic obstructive pulmonary disease (COPD) including emphysema and chronic bronchitis is a prevalent condition primarily associated with cigarette smoking (CS). Patients affected by emphysema often exhibit progressive respiratory symptoms and loss of lung function, which in many culminates in respiratory failure, as well as systemic symptoms of weight loss, which may lead to cachexia. We and other research groups have shown that exaggerated (capillary endothelial cell) apoptosis, which may occur in the context of a vascular endothelial growth factor (VEGF)-deprived environment (1), is one contributing mechanism of lung injury in emphysema and thus an important therapeutic target (1-4). Because adult mesenchymal precursor/stem cells of adipose tissue origin protect against apoptosis of endothelial cells from systemic vascular beds (5, 6), we investigated the ability of these adipose-derived stromal (stem) cells (ASC) to inhibit the death of lung endothelial cells *in vivo* and limit the lung injury induced by cigarette smoke.

There is increasing interest in exploiting the regenerative potential of stem cells to the treatment of lung diseases. Bone marrow (BM)-derived stem cells transplanted to the lungs can exhibit phenotypic and can acquire functional markers of airway or alveolar epithelial cells, interstitial cells and vascular endothelial cells (7). Potential lung protective and regenerative activities of both endothelial progenitor cells activated by the hepatocyte growth factor (HGF) and autologous ASC have been suggested in previous reports using an elastase-induced emphysema model (7, 8). Based on these findings, we sought to investigate in the context of cigarette smoke model the regenerative potential of human or murine ASC. ASC constitute a distinct progenitor cell population within the adipose stromal compartment that has the practical advantage of an easily accessible and ethically uncontested source, being obtained in large

numbers *via* liposuction from adults. The subcutaneous adipose tissue contains pluripotent cells in the stromal (non-adipose) compartment that can differentiate into multiple cell lineages, including neurons, skeletal myocytes, osteoblasts, chondroblasts, adipocytes, and vascular wall cells (9). Our previous studies demonstrated that the protective properties of ASC are at least in part attributable to their capability to secrete multiple pro-angiogenic and anti-apoptotic growth factors, including VEGF and HGF (10, 11), which act in a paracrine manner (11-14). In addition, ASC may directly partner with vascular endothelial cells to form vascular networks *via* a process of adult vasculogenesis (15). It is thus conceivable that ASC could home to regions of pulmonary endothelial injury and promote endothelial integrity both by secretion of anti-apoptotic factors and by direct support of the pulmonary endothelium as mural cells. To test these hypotheses, we utilized two established experimental models of CS exposure- and VEGF receptor (VEGFR) blockade-induced emphysema, which share with human emphysema characteristics such as alveolar apoptosis, oxidative stress, and alveolar space enlargement and destruction (3, 16, 17). In addition to damaging pulmonary structures and function, long-term CS triggers clinically important extra-pulmonary manifestations, including cardiovascular disease (18, 19), total body weight loss (20, 21), and decreased bone-marrow derived stem cell differentiation and migration potential (22, 23). While there has been significant progress in understanding the pathogenesis of and developing therapies for the CS-induced cardiovascular dysfunction, much less is known about the mechanisms by which CS affects body mass and bone marrow (BM) function, and no treatments exist for these conditions.

In the present study, intravenous administration of adult ASC of either human or mouse origin aimed at repairing the small vessel injury induced by CS or VEGFR inhibition improved both the pulmonary and systemic effects of CS in mice. These findings point the way to a new

potential therapeutic option for COPD and other diseases involving disruption of the pulmonary architecture.

METHODS

Reagents and antibodies. All chemical reagents were purchased from Sigma-Aldrich (St. Louis, MO), unless otherwise stated.

ASC harvesting, characterization, and culture. Human ASC were isolated from human subcutaneous adipose tissue samples obtained from liposuction procedures as previously described (24). Briefly, samples were digested in collagenase Type I solution (Worthington Biochemical, Lakewood, NJ) under agitation for 2 hours at 37°C, centrifuged at 300g for 8 minutes to separate the stromal cell fraction (pellet) from adipocytes. The pellets were filtered through 250 μ m Nitex filters (Sefar America Inc., Kansas City, MO) and treated with red cell lysis buffer (154mM NH_4Cl_2 , 10mM KHCO_3 , and 0.1mM EDTA). The final pellet was re-suspended and cultured in EGM-2mv (Lonza). ASC were passaged when 60-80% confluent and used at passage 3-6. Purity of ASC samples from endothelial cell contamination was confirmed by staining ASC monolayers with anti-CD31 antibodies. Mouse ASC were isolated in a similar fashion from adult DBA/2J, B6.129P2-*ApoE*^{*tm1Unc*}/J (Apo E), and B6;129S-Gt(ROSA)26Sor/J (“ROSA26”) mice (25). ASC were labeled *ex vivo*, prior to intravenous administration, with DiI, a lipophilic carbocyanine that fluoresces following incorporation into cell membranes, using the manufacturer’s protocol (Invitrogen). Morbidity or mortality from embolic lodging of ASC administration was not seen unless the number of ASC injected exceeded 5×10^5 , or the passage number of ASC expanded *ex vivo* exceeded 3 when a larger cellular size was noted, which prompted us to utilize mouse ASC up to passage 3, followed by filtration through a 40 μ m filter prior to injection.

Animal studies were approved by the Animal Care and Use Committee of Indiana University. C57Bl/6, ApoE, ROSA26, and DBA/2J mice were from Jackson Labs. At the end of experiments, the mice were euthanized and the tissue was processed as described (3). In addition, mice underwent bronchoalveolar lavage (BAL), utilizing PBS (0.6 ml). BAL cells were sedimented *via* centrifugation and counted after Giemsa staining of cytopins. The remaining acellular fluid was then snap-frozen in liquid nitrogen and stored at -80°C for further analysis.

***In vivo* CS exposure** was performed as previously described [40]. C57Bl/6 (female, age 12 weeks; n=5-10 per group) or DBA/2J (male; age 12-14 weeks; n=5-10 per group) mice were exposed to CS or ambient air for up to 24 weeks. Briefly, mice were exposed to 11% mainstream and 89% side-stream smoke from reference cigarettes (3R4F; Tobacco Research Institute, Kentucky) using a Teague 10E whole body exposure apparatus (Teague Enterprise, CA). The exposure chamber atmosphere was monitored for total suspended particulates (average 90 mg/m³) and carbon monoxide (average 350 ppm). In all CS experiments, mice were euthanized and lungs were processed as previously described (3) the day following the last day of CS exposure.

VEGF receptor blockade was performed as previously described (3). NOD.Cg-Prkdc^{scid} *IL2R γ ^{null}* (NS2) mice (Indiana University Cancer Center Stem Cell Core) (female; age 9 weeks;) were injected with SU5416 (Calbiochem; 20 mg/kg, subcutaneously) or vehicle, carboxymethylcellulose (CMC) and the mice were euthanized at the indicated time.

Lung disintegration and ASC detection by flow cytometry: Following euthanasia, the mouse trachea was cannulated and the thoracic cavity was opened. The lung vasculature was perfused with sterile PBS (20 ml; Invitrogen). The lung tissue was digested in 10% FBS in DMEM, 6.5µg/ml DNase I, and 12µg/ml Collagenase I (Roche) (30 min; shaking 200 rpm; 37°C). The cell suspension was strained through a 70µm cell strainer (Fisher Scientific) and cells were collected by

centrifugation (500 x g; 5 minutes; 4°C). Cells were resuspended in Geyes solution, centrifuged as before, and collected in PBS, followed by fixation with paraformaldehyde (1%; 30 minutes; 21°C). Cells were then collected by centrifugation (500 x g; 5 min; 21°C), and resuspended in PBS for flow cytometry. Thirty thousand cells were analyzed for the presence of Vybrant DiI (Molecular Probes V22885) using flow cytometry (FC 500; emission 575nm, excitation 488nm).

Cell death was detected in inflated fixed lung sections, enabling specific evaluation of alveoli, rather than large airways and vessels (26), *via* active caspase-3 IHC (Abcam and Cell Signaling) (3), using rat serum as negative control. The immunostaining for active caspase-3 was followed by DAPI (Molecular Probes) nuclear counter-staining. Executioner caspase (caspase-3 and/or -7) activity was measured with ApoONE homogeneous Caspase-3/7 assay kit (Promega, Madison, WI) as described (3). Human recombinant caspase-3 (Calbiochem) was utilized as positive control.

Immunohistochemistry (IHC). Paraffin sections, or for some applications, (GFP visualization) cryosections were blocked with 10% rabbit (or goat serum, if secondary antibody from goat) and incubated with primary antibodies or control antibodies. Anti-caspase-3 (Cell Signaling) antibody was incubated for 1 hour at room temperature or at 4°C overnight. Bound antibody was detected according to the manufacturer's instructions using a biotin-conjugated goat anti-rat IgG secondary antibody (Vector Laboratories, Burlingame, CA; 1:100) and Streptavidin-coupled phycoerythrin or FITC (Vector, 1:1000) were used. Sections were counterstained with DAPI and mounted with Mowiol 488 (Calbiochem). Microscopy was performed on either a Nikon Eclipse (TE200S) inverted fluorescence or a combined confocal/multi-photon (Spectraphysics laser, BioRad MRC1024MP) inverted system. Images were captured in a blinded fashion and quantitative intensity (expression) data was obtained by Metamorph Imaging software (Universal) as previously described (4).

Morphometric analysis was performed in a blinded fashion on coded slides as described, using a macro developed by Dr. Rubin M. Tuder (U Colorado) for Metamorph (26, 27).

Lung volume measurements were performed with the flexiVent system (Scireq, Montreal, Canada). Mice were anesthetized with inhaled isoflurane in oxygen and orotracheally intubated with a 20 gauge intravenous cannula under direct vision. A good seal was confirmed by stable airway pressure during a sustained inflation. Isoflurane anesthesia was maintained throughout the measurements, and the mice were hyperventilated to eliminate spontaneous ventilation.

Western blotting. Lung tissue was homogenized in RIPA buffer with protease inhibitors on ice and proteins were isolated by centrifugation at 16,000 X g for 10 minutes at 4°C. Proteins were loaded in equal amounts (10-30µg) as determined by BCA protein concentration assay (Pierce, Rockford, IL). Total proteins were separated by SDS-PAGE using Criterion gels (Bio-Rad) followed by immunoblotting. Briefly, samples were mixed with Laemmli buffer, heated at 95°C for 5 min and loaded onto 4-20% SDS-PAGE gels. Proteins were separated by electrophoresis and blotted onto PVDF membranes (Millipore). Non-specific binding was reduced by blocking the membrane in Protein Free Blocking buffer (Pierce) or TBS/0.1% tween-20/5% nonfat dry milk. Primary antibodies were diluted in a sodium phosphate buffer containing 50mM sodium phosphate, 150mM NaCl, 0.05% Tween-20, 4% BSA, and 1mM sodium azide. Primary antibodies and their dilutions are as follows: ERK1/2 (1:2000; Cell Signaling), phospho-ERK1/2 (1:1000; Cell Signaling), p38 (1:1000; Cell Signaling), phospho-p38 (1:1000; Cell Signaling), JNK (1:1000; Cell Signaling), phospho-JNK (1:1000; Cell Signaling), vinculin (1:5000; Calbiochem), or β-actin (1:30,000; Sigma). Blots were washed with TBS + 0.1%

Tween-20 and incubated with HRP-conjugated secondary antibodies to rabbit (1:10,000; Amersham; Piscataway, NJ) or mouse (1:10,000; Amersham) in 5% dry milk in TBST. Blots were detected using ECL-plus (Amersham) or SuperSignal (Pierce).

Hematopoietic Progenitor Cell Analysis. The absolute numbers and cell cycling status of granulocyte macrophage (CFU-GM), erythroid (BFU-E), and multipotential (CFU-GEMM) progenitor cells was calculated as previously reported (28, 29). In short, BM cells were flushed from femurs of control and treated mice, and nucleated cellularity calculated per femur. Femoral cells were treated *in vitro* with control medium, or high specific activity tritiated thymidine as a 30 minute pulse exposure, washed, and plated at 5×10^4 cells/ml in 1% methylcellulose culture medium with 30% fetal bovine serum (FBS, Hyclone, Logan, UT), and recombinant human erythropoietin (Epo, 1U/ml, Amgen Corp, Thousand Oaks, CA), recombinant murine stem cell factor (SCF, 50ng/ml, R & D Systems, Minneapolis, MN), and 5% vol/vol pokeweed mitogen mouse spleen cell conditional medium (29). Semi-solid cell cultures were placed in culture at 5% CO₂ at lowered (5%) O₂ in a humidified chamber, and CFU-GM-, BFU-E-, and CFU-GEMM-colonies scored after 7 days incubation. The number of colonies and femoral nucleated cellularity was used to calculate numbers of progenitors per femur. The high specific activity tritiated thymidine kill assay allows an estimate of the cell cycling status of progenitors by analysis of the percent progenitors in S-phase at time cells were removed from mice and plated (29).

Lung endothelial cells. Primary human lung microvascular endothelial cells were obtained from Lonza (Allendale, NJ) and maintained in culture medium consisting of EMB-2, 5% FBS, 0.4% hydrocortisone, 1.6% hFGF, 1% VEGF, 1% IGF-1, 1% ascorbic acid, 1% hEGF,

1% GA-100, and 1% heparin at 37°C in 5% CO₂ and 95% air. Experiments were performed up to passage 10 with cells at 80-100% confluence.

CS extract preparation. An aqueous CS extract was prepared from filtered research grade cigarettes (1R3F) from the Kentucky Tobacco Research and Development Center at the University of Kentucky. A stock (100%) CS extract was prepared by bubbling smoke from 2 cigarettes into 20 ml of basal culture medium (EBM2; Lonza) at a rate of 1 cigarette per minute to 0.5 cm above the filter, using a modified method developed by Carp and Janoff (30). The extract's pH was adjusted to 7.4, followed by filtration (0.2 µm, 25 mm Acrodisc; Pall, Ann Arbor, MI) and used in cell culture experiments within 20 min. A similar procedure was used to prepare the control extract, replacing the CS with ambient air.

Endothelial cell wound repair assays. Wounding of cultured cells was performed using the Electric Cell Impedance System (ECIS, Applied Biophysics; Troy, NY). Human lung microvascular endothelial cells were grown as detailed above on gold microelectrodes (8W1E) until confluent. Cells were pretreated for 2 hr in basal medium or in conditioned medium collected from cultured adult human ASC (50% v:v). Cells were then treated wounded *via* a linear electrical injury applied *via* ECIS, in the presence or absence of CS extract (4%). Wound repair was quantified by measuring cellular resistance over time and normalizing it to the time of wounding, reporting the slope of the TER recovery until monolayer confluence was achieved.

Statistical analysis was performed with SigmaStat software using ANOVA with Student-Newman-Keuls *post hoc* test, or Student's t-test. Statistical difference was accepted at $p < 0.05$.

RESULTS

ASC characterization and localization in the lungs following systemic delivery.

Initial studies of the distribution of ASC following systemic administration were conducted using ROSA26 mouse-derived ASC expressing β -galactosidase under the control of an unknown endogenous promoter delivered intravenously into non- β -galactosidase expressing mice bearing a homozygous deletion of the ApoE locus. Tissues of these animals were stained for β -galactosidase expression at 1, 7, and 21 days following delivery. Gross inspection 1h following administration revealed a predominantly pulmonary localization, with a pattern of distribution consistent with intravascular trapping (**Supplementary Figure 1A**), which was confirmed histologically by the presence ASC in the lung parenchyma in lac Z-ASC-treated wild-type mice which exhibited X-gal staining, compared to vehicle-injected control wild-type mice which lacked X-gal staining (**Figure 1A**). Interestingly, evaluation at 7 and 21 days following ASC delivery demonstrated focal areas of staining consistent with incorporation of lacZ-expressing cells in the airway epithelium, including that of medium and large-sized airways (**Figure 1A**).

In separate homing experiments, autologous GFP-labeled mouse ASC (3×10^5 cells) were administered systemically *via* intravenous injection to DBA/2J mice. Using immunohistochemistry, GFP-labeled cells were detected in the lung alongside resident cells in both large airway epithelial and sub-epithelial structures (**Supplementary Figure 1B**), as well as in parenchymal, vascular and alveolar structures at 1 week following their administration (**Supplementary Figure 1C**). To avoid potential immunostaining artifacts, interference with the lung autofluorescence, and to allow for a more quantitative assessment, Vybrant DiI -labeled

autologous ASC were injected into DBA2 mice followed by immunofluorescence microscopy on frozen lung sections at day 21 (**Figure 1B**) and the persistence of the labeled ASC was evaluated by flow cytometry of disintegrated lungs at days 1, 7, and 21 following a single injection of ASC (**Figure 1C, D**). DiI-labeled ASC were detected at 21 days using epifluorescence and confocal fluorescence microscopy in the lung parenchyma of ASC-injected mice, but not littermate mice injected with vehicle (**Figure 1B**). In contrast, evaluation of the BM of mice exposed to either ambient air or CS at 21 days after a single intravenous injection of DiI-labeled ASC revealed no significant trapping of ASC (data not shown). Consistent with our experience of initial retention of human ASC in the lung following systemic delivery in ApoE mice, the injected DiI-labeled mouse ASC were found in significantly higher numbers in the lungs at day 1, compared to 7 days or 21 days after injection ($p < 0.05$). Interestingly, exposure to CS for 2 weeks prior to ASC injection led to a decrease in lung trapping of ASC at 21 days (**Figure 1E**). It is not known whether the persistence of ASC in the lungs is required for their putative regenerative effects in the lung. Given this uncertainty, we next investigated whether repetitive injection of ASC was sufficient to prevent airspace enlargement in CS-induced emphysema, the disease model of highest clinical relevance. To ensure that all expected components of the emphysematous process, including inflammatory elements remained intact, for these studies we elected to employ DBA/2J mice with isogenic mouse-derived ASC.

Treatment with ASC decreased CS-induced lung inflammation, caspase activation, and airspace enlargement

DBA/2J mice were exposed to CS or ambient air for 4 months; while a third group of mice, also exposed to CS in parallel, were given ASC collected from littermate mice, expanded

ex vivo, and administered by intravenous injection every other week during the last 2 months of the 4 month CS exposure. In a second similar experiment, a fourth group of CS-exposed mice received ASC carrier, as a vehicle control. As expected, CS exposure (4 months) in the DBA/2J mice increased lung inflammation, measured by an elevated number of inflammatory cells (macrophages and polymorphonuclear cells) in the bronchoalveolar lavage (BAL) (**Figure 2A-B**), increased alveolar cell death, measured by caspase-3 activity and immunohistochemistry (**Figure 2C-E**), and caused significant alveolar space enlargement, measured by the standardized automated morphometry of alveolar structures on H/E-stained lung sections, when compared to control animals exposed to ambient air (**Figure 3**). In the group receiving systemic injections of ASC, there was an attenuation of the CS-induced increase in the number of macrophages and PMNs in the BAL (**Figure 2A-B**). ASC treatment attenuated the enzymatic activity of caspase-3 in total lung homogenates by more than 30% ($p=0.02$) (**Figure 2C**), and markedly decreased the CS- induced active caspase-3 expression in the lung parenchyma, measured by immunohistochemistry (**Figure 2D-E**) when compared to the CS-exposed mice who did not receive ASC or who only received vehicle control. These protective effects were associated with a significant decrease in alveolar space size compared to the group exposed to CS alone (**Figure 3A**), which was reflected by a significant decrease in the mean linear intercepts (MLI) from to $40.5 \pm 1 \mu\text{m}$ to $36.3 \pm 0.7 \mu\text{m}$ ($p=0.01$), a significant increase in alveolar surface area from $115.7 \pm 36 \text{ mm}^2$ to $280.1 \pm 34 \text{ mm}^2$ ($p=0.004$) (**Figure 3B**), and a significant attenuation of lung volume enlargement ($p=0.01$) (**Figure 3C**). The protective effects of ASC on lung inflammation, caspase activation, and alveolar integrity were associated with biochemical evidence of modulation of the CS-induced MAPK signal transduction pathways involved in inflammation

and apoptosis. Treatment with ASC abrogated the phosphorylation of p38 MAPK and attenuated JNK1 and AKT activities induced by the chronic CS exposure (**Supplementary Figure 2**).

Treatment with ASC prevented CS-induced weight loss in mice

As previously noted (20), chronic CS exposure caused a significant decrease in body weight, reaching 10% after 4 months of exposure ($p=0.003$) compared to mice of similar age and sex exposed to ambient air for the same duration of time (**Figure 4A**). Interestingly, CS-exposed mice treated with ASC during the last 2 months of exposure had no significant weight loss compared to ambient-air exposed control animals (**Figure 4A and Supplementary Figure 3**). When examined macroscopically, the area of fat measured from coded (blinded) photographs of abdominal subcutaneous region, the ASC-treated mice had a significant increase ($p<0.05$) in the abundance of subcutaneous fat compared to the untreated CS-exposed mice, (**Figure 4B-C**). Macroscopically, no difference in the body distribution of fat was noted compared to that in control mice (data not shown).

Treatment with ASC restored the BM dysfunction induced by CS in adult mice.

One of the less widely appreciated and studied systemic effect of CS exposure is the suppression of BM function (31, 32). To evaluate the capability of ASC to modulate the toxic effects of chronic CS exposure on hematopoiesis, BM was harvested from the femora of DBA/2J mice exposed to CS for 4 months that received either control carrier or ASC. CS exposure resulted in a marked and significant reduction in absolute numbers of bone marrow CFU-GM, BFU-E and CFU-GEMM, with these progenitors being in a slow or non-cycling state. In stark

contrast, ASC treatment during the last 2 months of CS exposure fully or nearly completely counteracted the suppressive effects of CS on BM function (**Figure 5 A-D**).

Treatment with human ASC decreased VEGFR inhibitor-induced airspace enlargement in immunodeficient mice.

The mechanism(s) by which ASC exerted their protective local and systemic effects in the CS model may include paracrine release of survival and growth factors, including VEGF (33, 34), which oppose the excessive apoptosis noted in response to CS exposure. To address this hypothesis, we next utilized a complementary model of emphysema driven by apoptosis due to decreased VEGF availability. We have previously demonstrated that VEGFR blockade with SU5416 (20 mg/kg; subcutaneously) caused significant increases in airspace enlargement in C57Bl/6 mice that peaked at 28 days (3). This airspace enlargement is dependent on alveolar cell apoptosis (1, 3), detected not only in endothelial but also in epithelial cell types (3), making this model ideally suited to address whether ASC treatment is sufficient to overcome a VEGF-deprived state and influence endothelial survival. In addition, to investigate whether not only the mouse, but also the human adult ASC are efficient at protecting against lung apoptosis, we employed immunodeficient Nod-SCID interleukin 2 receptor gamma chain-deficient (NS2) mice. Pilot experiments using this mouse demonstrated that the immunotolerant NS2 mouse is susceptible to development of airspace enlargement as a result of VEGFR blockade. Indeed, administration of SU5416 (20 mg/kg, subcutaneously) showed the NS2 mice exhibited a significant increase in alveolar enlargement at 21 days compared to vehicle (carboxymethylcellulose (CMC) controls in both male and female adult mice (data not shown).

Since systemically delivered ASC preferentially lodge and engraft in the lungs of mice 24 h following systemic delivery, we administered human ASC (3×10^5 cells; intravenous injection) at day 3 following VEGFR inhibition in adult NS2 female mice, a time at which lung apoptosis is increasing in this model, peaking between 3-7 days of VEGFR administration (3). GFP-labeled human ASC were detected in the lungs of NS2 mice 3 days after injection (day 6 of VEGFR blockade), as determined by GFP immunoblotting of total lung homogenates (**Supplementary Figure 1B**). At 28 days, the VEGFR blockade-induced increase in cell death, measured by image analysis and quantification of the immunohistochemical expression of active caspase-3 in the lung parenchyma was significantly attenuated by 75% ($p=0.03$) following treatment with a single injection of human adult ASC (**Figure 6A-B**). Furthermore, the VEGFR-blockade-induced alveolar enlargement was significantly decreased, measured by a 70% improvement ($p=0.006$) in mean linear intercepts following the systemic administration of human adult ASC (**Figure 6C**). These results suggested ASC have prominent protective anti-apoptotic effects in the lung, thus, overcoming the specific effects of VEGF inhibition.

Human ASC-conditioned medium improved the repair of lung endothelial cells monolayers *in vitro*

To identify if ASC are capable of providing a protective effect towards injured lung microvascular endothelial cells specifically *via* a paracrine mechanism, we studied adult human ASC-conditioned medium (ASC-CM) in an *in vitro* model of lung endothelial injury. The integrity of the normally tight cultured lung endothelial cell monolayers can be tracked in real time by measuring the trans-endothelial electrical resistance (TER) of cells grown on microelectrodes, utilizing the electrical cell impedance system (ECIS). Utilizing this approach,

we studied the effect of ASC-CM on lung endothelial cell wound repair following wounding induced by a linear electrical injury applied through microelectrodes in contact with the monolayer. Following wounding, which is characterized by a sudden decrease in TER, the monolayer repairs *via* both cell growth and migration of endothelial cells from the wound edges towards the “wound” (35), which is reflected by a gradual restoration of TER towards that of confluent monolayers. Cell monolayers grown at confluence were “wounded” *via* a linear electrical injury applied through microelectrodes in contact with the monolayer. Pretreatment of primary human lung microvascular endothelial cell monolayers with ASC-CM significantly ($p=0.003$) enhanced the TER recovery following wounding compared to untreated cells (**Figure 7 A-B**). Interestingly, in the presence of a CS extract, which contains the water soluble fraction of CS that mimics its circulating components, there was a marked delay in lung endothelial cell wound healing (**Figure 7A, C**); both the slope of TER recovery and the absolute TER attained at full recovery following wounding were significantly blunted compared with wounded endothelial cells exposed to ambient air-extract control. Strikingly, endothelial cell monolayers repaired the wound significantly faster in the presence of ASC-CM, even during concomitant CS extract exposure (**Figure 7A**). Since the ASC-CM contains serum necessary for their growth, and since serum itself has numerous growth factors, we investigated the effect of the control conditioned medium which contained serum on wound repair. Although serum exerted a marked protective effect on the slope of wound repair, only cells treated with ASC-CM sustained their monolayer barrier function attained following wounding (**Figure 7B-C**). These data suggest that factors secreted by ASC exert protective effects against lung endothelial cell damage and may antagonize the injurious effects of CS exposure.

DISCUSSION

These results demonstrate that both murine and human ASC are capable of significantly ameliorating the pulmonary damage caused by CS exposure, even when administered mid-way during a temporally protracted CS exposure. The observed profound protective effects of ASC in the murine lung, as well as the vascular protective properties of paracrine factors secreted by these cells render such therapy a potentially promising intervention in emphysema. Recognition of the importance of endothelial apoptosis in experimental pulmonary emphysema (1, 3, 4), including following tobacco smoke exposure (36, 37), has prompted a focus on the potential role for vascular cell-responsive growth factor modulation as a novel approach to treatment. Models involving endothelial apoptosis caused by either exposure to CS or specific impairment of endothelial survival by VEGFR-blockade allow the evaluation of putative therapies in the context of a clinically relevant toxic exposure and a specific molecular lesion, respectively. Our previous demonstration that ASC can elicit both angiogenic and anti-apoptotic effects in multiple systems (5, 6, 14) led us to hypothesize that the systemic administration of ASC may help to restore damaged pulmonary capillary networks and also may serve to protect the alveolar architecture from destruction in these models of emphysema. Prior studies have shown that both intravenous systemic administration of ASC and local placement of ASC on a synthetic scaffold could limit the extent of elastase-induced emphysema and accelerate lung growth after experimental lung volume reduction surgery in rats (38-40), but have not investigated their activity in the context of CS exposure.

The therapeutic effects of ASC on the pulmonary system may engage multiple mechanisms, including secretion of anti-apoptotic factors with paracrine protective action on

neighboring resident lung cells, activation of endogenous progenitor cell cycling and differentiation, rescue and recruitment of circulating cells engaged in pulmonary repair, and direct differentiation into pulmonary epithelial or endothelial cells. The relatively low number of ASC detectable in lung tissue several days following administration, coupled with their effective anti-apoptotic and overall lung protective effects, suggest that an important therapeutic function of ASC may be to promote endogenous repair processes and limit damage through paracrine effects. Similar protective effects of ASC delivery in the VEGF-inhibition model of emphysema supports the notion that VEGF is one of the factors secreted by ASC which exert protective effects on lung endothelial cells, much as we have described previously in the context of cultured endothelial cells (10). However, the paracrine effects of ASC on cultured lung endothelium, while corroborative, cannot be directly extrapolated to complex animal models of CS-induced emphysema and therefore more studies are needed to define the extent to which these paracrine effects may occur in vivo. Such paracrine effects may be combined with a direct cellular integration of ASC among other structural components of the lung, a scenario suggested by the detection of ASC for up to 3 weeks following injection, intercalated among alveolar cells in the parenchyma and among epithelial cells in large airways. While the relevance of this integration is not yet established, it is possible that ASC may be directly participating in tissue regeneration to limit CS-induced lung injury.

Our data revealed a novel function of adult ASC in promoting the repair of the lung endothelial barrier function, even in the presence of CS. These vascular protective properties of ASC are in agreement with previous reports of bone-marrow derived progenitor stem cells that can reduce lung vascular permeability (41) and may be explained by their endogenous localization in the adipose tissue in a perivascular niche, where they exhibit pre-pericytes

markers (24). Furthermore, ASC secrete potent pro-survival factors and ASC-CM has exert anti-apoptotic effects on systemic vascular endothelial cells, which has been shown to be predominantly mediated through the actions HGF and VEGF on angiogenesis and the formation of new vessels (33).

Remarkably, the marked effects of chronic CS exposure on body weight, adipose depots, and hematopoietic progenitor cycling and colony formation of multiple BM colony-forming types were substantially reversed by ASC, demonstrating that the provision of ASC results in systemic protection against diverse pathologies induced by such smoke exposure. Substantial weight loss in the context of cigarette smoking is a well-known clinical phenomenon and described previously in C57/Bl6 mice exposed to CS for 9 weeks (20, 21). We noted a similar effect of CS in the DBA/2J mice. The weight loss (cachexia) associated with advanced stages of COPD portends a poor prognosis for these patients, even after smoking cessation, and has no effective treatment. Therefore, the ability of the ASC to reverse the weight loss may be of great therapeutic promise, although the mechanisms of action and the cell-type specificity of this effect remain to be determined. It is interesting that such cachexia may be the result of excessive circulating TNF- α levels (42). In fact a recent study of BM-derived mesenchymal stem cells (BM-MSC), which bear substantial similarity to ASC (43, 44), demonstrated that BM-MSC, which also predominantly localized in the lung following intravenous administration, promote systemic tissue repair by secreting several specific molecules in response to elevated levels of circulating TNF- α found in the context of tissue damage (45). It is intriguing to speculate that such a TNF- α mediated activation of ASC may likewise induce secretion of a spectrum of molecules that block the cachectic effects of TNF- α .

The BM is the main adult repository for hematopoietic stem cells and an important source for endothelial progenitors; and each of these populations has been reported to be depressed due to CS or nicotine, a major component of CS (22, 23, 32). In addition, reports by Liu *et al*, among others, have noted that CS causes the release of immature eosinophils from BM and that Balb/c mice exposed to nicotine demonstrate impairment of hematopoietic stem cell migration, which is hypothesized to alter stem cell homing (31, 32, 46). Further *in vitro* data have demonstrated that CS extract strikingly diminishes BM progenitor cell chemotaxis in Boyden chamber assays. Our analysis of the BM from mice exposed to CS revealed that BM-derived progenitor cells had diminished proliferation capacity and were decreased in number. It remains to be shown whether these progenitor cells might be mediators of ASC-induced lung protection and whether their inhibition due to CS exposure could contribute to inability to repair the lung parenchyma in COPD. Should that be the case, ASC-induced restoration of BM progenitor cell cycling and numbers might constitute a novel mechanism by which these cells exert vascular protective effects. The mechanism by which administration of ASC restored the proliferation of the hematopoietic progenitor cells remains unknown, but could potentially involve molecules that overlap with those active in sustaining body mass as described above. Identification of these mechanisms will be helpful both in defining approaches to ASC therapeutic use as well as for potentially pointing the way to new molecular targets for therapeutic intervention in pulmonary emphysema.

In conclusion, adult ASC exert protective properties against lung endothelial injury and against pulmonary and systemic deleterious effects of CS exposure, including airspace enlargement, weight loss, and BM suppression. These cells, which are a readily available population of highly proliferative and clonogenic cells resident in the stromal fraction of adipose

tissues and may be readily expanded *in vitro* may represent a potential therapeutic option in lung diseases characterized by excessive apoptosis, including pulmonary emphysema.

Acknowledgements: We thank Yuan Gu, Dr. Adetayo R. Ademuyiwa, Todd Cook, Yong Gao, and Osato Ogbeifun for technical support.

Cited literature

1. Kasahara Y, Tudor RM, Taraseviciene-Stewart L, Le Cras TD, Abman S, Hirth PK, Waltenberger J, Voelkel NF. Inhibition of vegf receptors causes lung cell apoptosis and emphysema. *J Clin Invest* 2000;106:1311-1319.
2. Diab KJ, Adamowicz JJ, Kamocki K, Rush NI, Garrison J, Gu Y, Schweitzer KS, Skobeleva A, Rajashekhar G, Hubbard WC, et al. Stimulation of sphingosine 1 phosphate signaling as an alveolar cell survival strategy in emphysema. *Am J Respir Crit Care Med* 2009.
3. Petrache I, Natarajan V, Zhen L, Medler TR, Richter AT, Cho C, Hubbard WC, Berdyshev EV, Tudor RM. Ceramide upregulation causes pulmonary cell apoptosis and emphysema-like disease in mice. *Nat Med* 2005;11:491-498.
4. Giordano RJ, Lahdenranta J, Zhen L, Chukwueke U, Petrache I, Langley RR, Fidler IJ, Pasqualini R, Tudor RM, Arap W. Targeted induction of lung endothelial cell apoptosis causes emphysema-like changes in the mouse. *J Biol Chem* 2008;283:29447-29460.
5. Cai L, Johnstone BH, Cook TG, Liang Z, Traktuev D, Cornetta K, Ingram DA, Rosen ED, March KL. Suppression of hepatocyte growth factor production impairs the ability of adipose-derived stem cells to promote ischemic tissue revascularization. *Stem Cells* 2007;25:3234-3243.

6. Wei X, Du Z, Zhao L, Feng D, Wei G, He Y, Tan J, Lee WH, Hampel H, Dodel R, et al. Ifats collection: The conditioned media of adipose stromal cells protect against hypoxia-ischemia-induced brain damage in neonatal rats. *Stem Cells* 2009;27:478-488.
7. Ishizawa K, Kubo H, Yamada M, Kobayashi S, Numasaki M, Ueda S, Suzuki T, Sasaki H. Bone marrow-derived cells contribute to lung regeneration after elastase-induced pulmonary emphysema. *FEBS Lett* 2004;556:249-252.
8. Shigemura N, Okumura M, Mizuno S, Imanishi Y, Nakamura T, Sawa Y. Autologous transplantation of adipose tissue-derived stromal cells ameliorates pulmonary emphysema. *Am J Transplant* 2006;6:2592-2600.
9. Zuk PA, Zhu M, Mizuno H, Huang J, Futrell JW, Katz AJ, Benhaim P, Lorenz HP, Hedrick MH. Multilineage cells from human adipose tissue: Implications for cell-based therapies. *Tissue Eng* 2001;7:211-228.
10. Rehman J, Li J, Parvathaneni L, Karlsson G, Panchal VR, Temm CJ, Mahenthiran J, March KL. Exercise acutely increases circulating endothelial progenitor cells and monocyte/macrophage-derived angiogenic cells. *J Am Coll Cardiol* 2004;43:2314-2318.
11. Rajashekhar G, Traktuev DO, Roell WC, Johnstone BH, Merfeld-Clauss S, Van Natta B, Rosen ED, March KL, Clauss M. Ifats collection: Adipose stromal cell differentiation is reduced by endothelial cell contact and paracrine communication: Role of canonical wnt signaling. *Stem Cells* 2008;26:2674-2681.

12. Cai L, Johnstone BH, Cook TG, Tan J, Fishbein MC, Chen PS, March KL. Ifats collection: Human adipose tissue-derived stem cells induce angiogenesis and nerve sprouting following myocardial infarction, in conjunction with potent preservation of cardiac function. *Stem Cells* 2009;27:230-237.
13. Rodriguez AM, Pisani D, Dechesne CA, Turc-Carel C, Kurzenne JY, Wdziekonski B, Villageois A, Bagnis C, Breittmayer JP, Groux H, et al. Transplantation of a multipotent cell population from human adipose tissue induces dystrophin expression in the immunocompetent mdx mouse. *J Exp Med* 2005;201:1397-1405.
14. Wei X, Zhao L, Zhong J, Gu H, Feng D, Johnstone BH, March KL, Farlow MR, Du Y. Adipose stromal cells-secreted neuroprotective media against neuronal apoptosis. *Neurosci Lett* 2009;462:76-79.
15. Traktuev DO, Prater DN, Merfeld-Clauss S, Sanjeevaiah AR, Saadatzadeh MR, Murphy M, Johnstone BH, Ingram DA, March KL. Robust functional vascular network formation in vivo by cooperation of adipose progenitor and endothelial cells. *Circ Res* 2009;104:1410-1420.
16. Guerassimov A, Hoshino Y, Takubo Y, Turcotte A, Yamamoto M, Ghezzi H, Triantafillopoulos A, Whittaker K, Hoidal JR, Cosio MG. The development of emphysema in cigarette smoke-exposed mice is strain dependent. *Am J Respir Crit Care Med* 2004;170:974-980.

17. Bartalesi B, Cavarra E, Fineschi S, Lucattelli M, Lunghi B, Martorana PA, Lungarella G. Different lung responses to cigarette smoke in two strains of mice sensitive to oxidants. *Eur Respir J* 2005;25:15-22.
18. Agusti AG, Noguera A, Sauleda J, Sala E, Pons J, Busquets X. Systemic effects of chronic obstructive pulmonary disease. *Eur Respir J* 2003;21:347-360.
19. Oudijk EJ, Lammers JW, Koenderman L. Systemic inflammation in chronic obstructive pulmonary disease. *Eur Respir J Suppl* 2003;46:5s-13s.
20. Gosker HR, Langen RC, Bracke KR, Joos GF, Brusselle GG, Steele C, Ward KA, Wouters EF, Schols AM. Extrapulmonary manifestations of chronic obstructive pulmonary disease in a mouse model of chronic cigarette smoke exposure. *Am J Respir Cell Mol Biol* 2009;40:710-716.
21. Rabkin S, Boyko, E., Streja, D. Relationship of weight loss and cigarette smoking to changes in high-density lipoprotein cholesterol. *The American Journal of Clinical Nutrition* 1981;34:1764-1768.
22. Seroby N, Orlovskaya I, Kozlov V, Khaldoyanidi SK. Exposure to nicotine during gestation interferes with the colonization of fetal bone marrow by hematopoietic stem/progenitor cells. *Stem Cells Dev* 2005;14:81-91.

23. Serobyán N, Schraufstatter IU, Strongin A, Khaldoyanidi SK. Nicotinic acetylcholine receptor-mediated stimulation of endothelial cells results in the arrest of haematopoietic progenitor cells on endothelium. *Br J Haematol* 2005;129:257-265.
24. Traktuev DO, Merfeld-Clauss S, Li J, Kolonin M, Arap W, Pasqualini R, Johnstone BH, March KL. A population of multipotent cd34-positive adipose stromal cells share pericyte and mesenchymal surface markers, reside in a periendothelial location, and stabilize endothelial networks. *Circ Res* 2008;102:77-85.
25. Soriano P. Generalized lacz expression with the rosa26 cre reporter strain. *Nat Genet* 1999;21:70-71.
26. Tudor RM, Zhen L, Cho CY, Taraseviciene-Stewart L, Kasahara Y, Salvemini D, Voelkel NF, Flores SC. Oxidative stress and apoptosis interact and cause emphysema due to vascular endothelial growth factor receptor blockade. *Am J Respir Cell Mol Biol* 2003;29:88-97.
27. Aherne WA, Dunnill MS. Morphometry. London: E. Arnold; 1982.
28. Broxmeyer HE, Orschell CM, Clapp DW, Hangoc G, Cooper S, Plett PA, Liles WC, Li X, Graham-Evans B, Campbell TB, et al. Rapid mobilization of murine and human hematopoietic stem and progenitor cells with amd3100, a cxcr4 antagonist. *J Exp Med* 2005;201:1307-1318.

29. Cooper S, and Broxmeyer, H.E. Measurement of interleukin-3 and other hematopoietic growth factors, such as gm-csf, g-csf, m-csf, erythropoietin and the potent co-stimulating cytokines steel factor and flt-3 ligand. . New York). John Wiley & Sons, Inc. ; 1996.
30. Carp H, Janoff A. Inactivation of bronchial mucous proteinase inhibitor by cigarette smoke and phagocyte-derived oxidants. *Exp Lung Res* 1980;1:225-237.
31. Liu X, Kohyama T, Kobayashi T, Abe S, Kim H, Reed EC, Rennard SI. Cigarette smoke extract inhibits chemotaxis and collagen gel contraction mediated by human bone marrow osteoprogenitor cells and osteoblast-like cells. *Osteoporos Int* 2003;14:235-242.
32. Pandit TS, Sikora L, Muralidhar G, Rao SP, Sriramarao P. Sustained exposure to nicotine leads to extramedullary hematopoiesis in the spleen. *Stem Cells* 2006;24:2373-2381.
33. Lee EY, Xia, Y., Kim, W., Kim, M., Kim, T., Kim, K., Park, B., Sung, J. Hypoxia-enhanced wound-healing function of adipose-derived stem cells: Increase in stem cell proliferation and up-regulation of vegf and bfgf. *Wound Repair and Regeneration* 2009;17:540-547.
34. Wang JH, Liu N, Du HW, Weng JS, Chen RH, Xiao YC, Zhang YX. [effects of adipose-derived stem cell transplantation on the angiogenesis and the expression of bfgf and vegf in the brain post focal cerebral ischemia in rats.]. *Xi Bao Yu Fen Zi Mian Yi Xue Za Zhi* 2008;24:958-961.

35. Moy AB, Van Engelenhoven J, Bodmer J, Kamath J, Keese C, Giaever I, Shasby S, Shasby DM. Histamine and thrombin modulate endothelial focal adhesion through centripetal and centrifugal forces. *J Clin Invest* 1996;97:1020-1027.
36. Rangasamy T, Cho CY, Thimmulappa RK, Zhen L, Srisuma SS, Kensler TW, Yamamoto M, Petrache I, Tuder RM, Biswal S. Genetic ablation of nrf2 enhances susceptibility to cigarette smoke-induced emphysema in mice. *J Clin Invest* 2004;114:1248-1259.
37. Kang MJ, Lee CG, Cho SJ, Homer RJ, Elias JA. Ifn-gamma-dependent DNA injury and/or apoptosis are critical in cigarette smoke-induced murine emphysema. *Proc Am Thorac Soc* 2006;3:517-518.
38. Hoffman AM, Shifren A, Mazan MR, Gruntman AM, Lascola KM, Nolen-Walston R, Kim CF, Tsai L, Pierce RA, Mecham RP, et al. Matrix modulation of compensatory lung regrowth and progenitor cell proliferation in mice. *Am J Physiol Lung Cell Mol Physiol* 2009.
39. Hegab AE, Kubo H, Yamaya M, Asada M, He M, Fujino N, Mizuno S, Nakamura T. Intranasal hgf administration ameliorates the physiologic and morphologic changes in lung emphysema. *Mol Ther* 2008;16:1417-1426.
40. Shigemura N, Okumura M, Mizuno S, Imanishi Y, Matsuyama A, Shiono H, Nakamura T, Sawa Y. Lung tissue engineering technique with adipose stromal cells improves surgical outcome for pulmonary emphysema. *Am J Respir Crit Care Med* 2006;174:1199-1205.

41. Zhao Y, Ohkawara, H., Rehman, J., Wary, K., Vogel, S., Minshall, R., Zhao, Y., Malik, A. Bone marrow progenitor cells induce endothelial adherens junction integrity by sphingosine-1-phosphate-mediated rac1 and cdc42 signaling. *Circ Res* 2009;105:696-704.
42. Di Francia M, Barbier D, Mege JL, Orehek J. Tumor necrosis factor-alpha levels and weight loss in chronic obstructive pulmonary disease. *Am J Respir Crit Care Med* 1994;150:1453-1455.
43. Gimble J, Guilak F. Adipose-derived adult stem cells: Isolation, characterization, and differentiation potential. *Cytotherapy* 2003;5:362-369.
44. Aust L, Devlin B, Foster SJ, Halvorsen YD, Hicok K, du Laney T, Sen A, Willingmyre GD, Gimble JM. Yield of human adipose-derived adult stem cells from liposuction aspirates. *Cytotherapy* 2004;6:7-14.
45. Lee RH, Pulin AA, Seo MJ, Kota DJ, Ylostalo J, Larson BL, Semprun-Prieto L, Delafontaine P, Prockop DJ. Intravenous hmscs improve myocardial infarction in mice because cells embolized in lung are activated to secrete the anti-inflammatory protein tsg-6. *Cell Stem Cell* 2009;5:54-63.
46. Van Eeden S, Yeung A, Quinlam K, Hogg JC. Systemic response to ambient particulate matter relevance to chronic obstructive pulmonary disease. *Proc Am Thorac Soc* 2005;2:61-67.

FIGURE LEGENDS

Figure 1. Lung homing of adult ASC delivered by intravenous administration to mice. A.

Localization of B-galactosidase-expressing murine ASC (blue) on lung sections imaged at the indicated magnification following fixation and staining with X-Gal and hematoxyllin. Lungs of Apo E mice were harvested at the indicated time (1h, 7d, and 21d) following 5×10^5 ASC or control vehicle (Ctl) administration. Note (arrows) the presence of ASC in the lung parenchyma (1h) and among the bronchial epithelial layer (7d and 21d). **B.** Epi-fluorescence (i; inset) and confocal fluorescence (ii) micrographs of frozen-sectioned lungs from DBA2 mice harvested 21 days following a single injection with DiI-labeled ASC (3×10^5) or vehicle (controls) and stained with DAPI (blue). Note peri-nuclear red fluorescence (arrows) in the ASC-injected mice, as well as green autofluorescence of elastin structures in the lung (arrowheads; i). **C.** Abundance of DiI-labeled murine ASC detected by flow cytometry of whole lung homogenates obtained by digestion and disintegration. Lungs were harvested 1, 7, and 21-days following ASC administration (3×10^5) or vehicle in DBA/2J mice previously exposed to CS for 2 weeks. All ASC groups $p < 0.05$ versus vehicle control; $*p < 0.05$ vs. day1; $n = 4-5$; ANOVA. **D.** Abundance of cell events consistent with DiI-labeled murine ASC detected by flow cytometry of lung homogenates harvested 21-days following a single ASC administration (3×10^5) or vehicle in DBA/2J mice previously exposed to CS or air control (AC) for 2 weeks. Mean + SEM; $*p < 0.05$ vs. AC; $n = 4-5$.

Figure 2. Effect of ASC treatment on CS- induced inflammation and caspase activation. A-B. Abundance of inflammatory cells alveolar macrophages (A) and polymorphonuclear cells (B) in the bronchoalveolar lavage (BAL) fluid collected from DBA/2J mice exposed to CS or ambient air (Air) for 4 months (n=8-12/ group) and treated with ASCs (3×10^5 cells infused intravenously every other week, during the month 3 and 4 of CS exposure). *p<0.05 versus control; #p<0.05 versus CS; ANOVA. **C-E.** Lung cell death was quantified in the same experiment by caspase-3 activity measured with a fluorimetric enzymatic kinetic assay and normalized by protein concentration in lung homogenates (C; mean + SEM; *p<0.05 versus vehicle control; ANOVA) and by abundance of active caspase-3-expressing cells in lung parenchyma measured (D; median box plot; arbitrary units (AU); *p<0.05 versus air control; #p<0.05 versus CS; ANOVA) by automated image analysis of lung sections immunostained with a specific antibody (E).

Figure 3. Effect of ASC treatment on CS- induced airspace enlargement. A. Alveolar airspaces stained with hematoxylin/eosin on fixed lung sections from mice exposed to CS or ambient air for 4 months. DBA/2J mice were treated with ASC (3×10^5 cells per injection, injected intravenously every other week), during the month 3 and 4 of CS exposure. Note the increased airspaces in the CS-exposed mice and the smaller airspaces in the CS-exposed mice treated with ASC. **B.** Alveolar surface area calculated by standardized morphometry of alveolar spaces on coded slides (mean + SEM; *p<0.05 versus air control; #p<0.05 versus CS; ANOVA). **C.** Lung volumes measured in anesthetized and intubated DBA/2J mice (n=5-10) at 4 months following CS exposure (mean + SEM; *p<0.05 versus air control; #p<0.05 versus CS; ANOVA).

Figure 4. Effect of ASC treatment on CS- induced weight loss in mice. A. Body weight of DBA/2J mice following 4 months of air or CS exposure. A third group was treated with ASC (3×10^5 cells per injection, injected intravenously every other week), during the month 3 and 4 of CS exposure. (mean +SEM; n= 10-12 *p<0.05 versus air control; #p<0.05 versus CS; ANOVA). **A-B.** Abundance of abdominal fat (A; mean +SEM; n= 3-6 *p<0.05 versus air control; #p<0.05 versus CS; ANOVA), measured 4 months. **B.** Note the marked decrease in the amount of abdominal fat in the CS-exposed mice (double arrows), compared to control mice and to ASC-treated CS-exposed mice (arrows).

Figure 5. Effect of ASC treatment on CS- induced bone marrow (BM) dysfunction in mice. Absolute numbers of nucleated cells (A), and hematopoietic progenitors: colony forming unit-granulocyte, monocyte, CFU-GM (B), burst-forming unit-erythroid, BFU-E (C), colony forming unit-granulocyte, erythrocyte, monocyte, and megakaryocyte, CFU-GEMM (D), and cycling status (= percent cells in S-phase) of these progenitors (E) in DBA/2J mice following 4 months of air or CS exposure, with a third group treated with ASC (3×10^5 cells per injection, injected intravenously every other week), during the month 3 and 4 of CS exposure (mean +SEM; n= 4-6; *p<0.05 versus air control; #p<0.005 versus CS; ANOVA).

Figure 6. ASC efficacy in an apoptosis-dependent alveolar enlargement model. A-B. Lung cell death was quantified by abundance of active caspase-3-expressing cells in lung parenchyma (at 4 weeks) in animals (Nod-SCID NS2 mice) who received a single dose of VEGF receptor inhibitor (SU5416, 20 mg/kg; sq) or its vehicle control (CMC), and who were treated with human adult ASC (3×10^5 , intravenous injection) on day 3 following VEGFR inhibition; (A;

mean arbitrary units (AU) + SEM; * $p < 0.05$ versus vehicle (control); # $p < 0.05$ versus ASC-untreated (-) animals who received the VEGFR-inhibitor; ANOVA). Quantification was achieved by automated image analysis of coded lung sections immunostained with a specific active caspase-3 antibody (B; brown; arrows). C. Mean linear intercepts calculated by standardized morphometry of alveolar spaces on coded slides of alveolar airspaces stained with hematoxylin/eosin on fixed lung sections from mice exposed to CMC vehicle or VEGFR-inhibitor air for 24 weeks and treated with ASC as above. (mean + SEM; * $p < 0.05$ versus CMC control; # $p < 0.05$ versus VEGFR-inhibited mice; ANOVA).

Figure 7. Paracrine effects of ASC on lung endothelia injury in vitro. A-C. Wound injury repair measured by the recovery of trans-cellular electrical resistance (TER) across a confluent monolayer of primary human lung microvascular endothelial cells grown on gold microelectrodes using the Electric Cell-Substrate Impedance Sensing (ECIS) system. A linear electrical injury was applied at time 2.4h (B-C, arrow) and the slope of TER recovery to plateau was compared for cells maintained in their regular growth medium, or in medium supplemented with conditioned medium from ASC cells (ASC-CM; 50%), in the absence and presence of CS extract (4%); A; boxplot with medians; $n = 4$ independent experiments; $p < 0.01$ 2-Way ANOVA for the effect of CS and ASC-CM; * $p < 0.005$ versus untreated wounded control cells; # $p < 0.005$ versus untreated wounded CS-exposed cells. B. Kinetics of normalized TER (to the TER at time of wound application) (mean; $n = 3-4$ independent experiments) in unexposed cells (i) or in cells exposed to CS (ii) wounded at time 2.4h (arrow), which were either untreated, grown in their control medium (Ctl; black line), or treated with ASC-CM (green line) or with control serum-containing media (FBS-CM, 20%; red line). Note the effect of CS extract on both the slope and

the attained plateau levels of TER recovery in wounded lung endothelial cells and the protective effects of both ASC-CM and serum on the slope of TER recovery, with ASC-CM-specific effects on the plateau TER, evident in panel (iii) which combines conditions shown in panels i and ii.

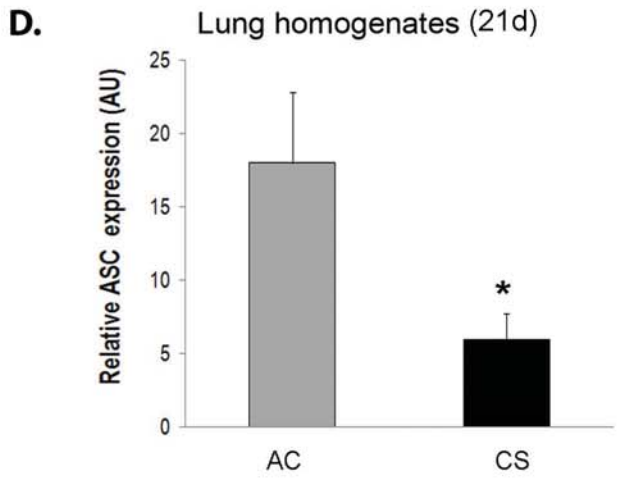
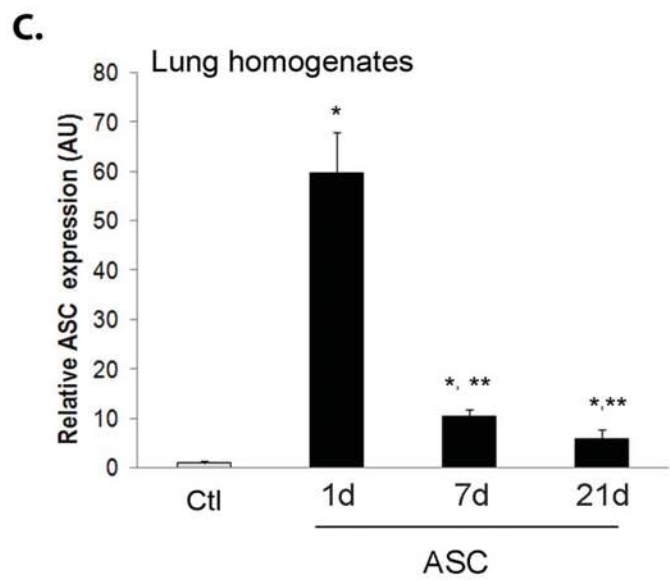
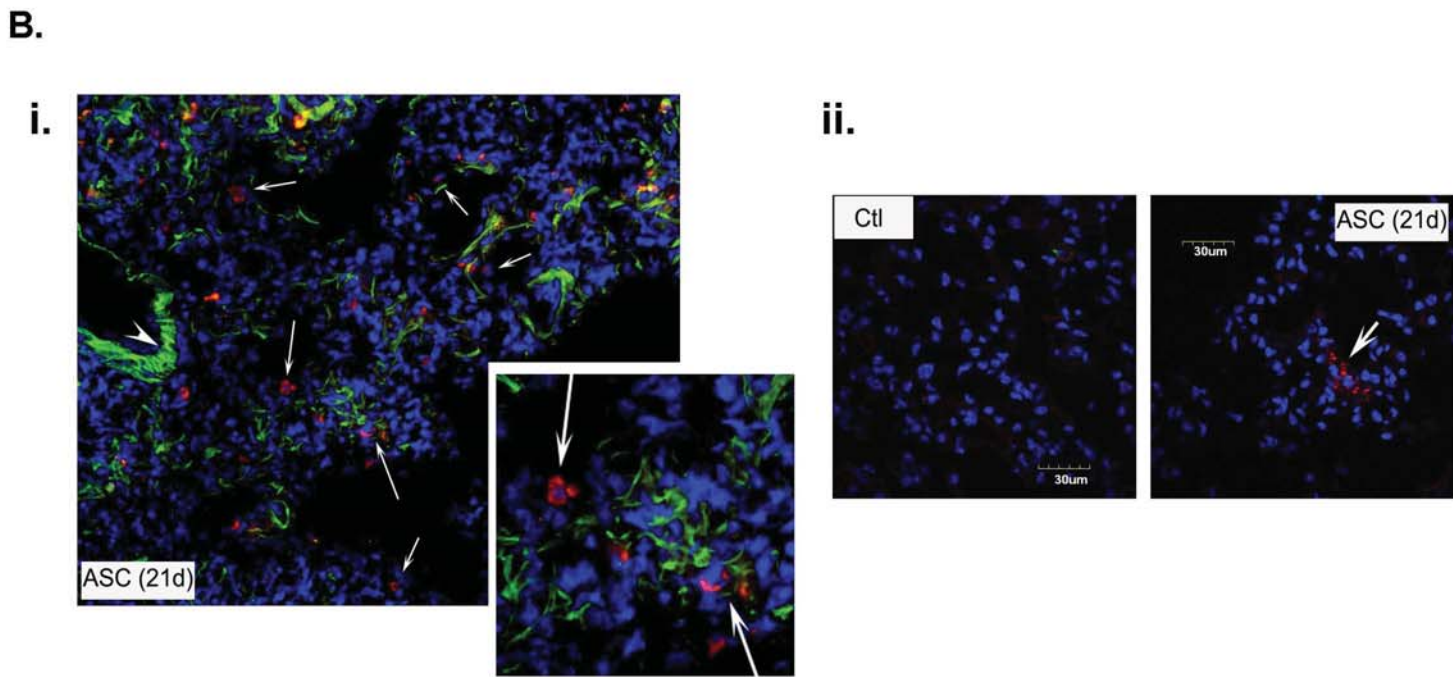
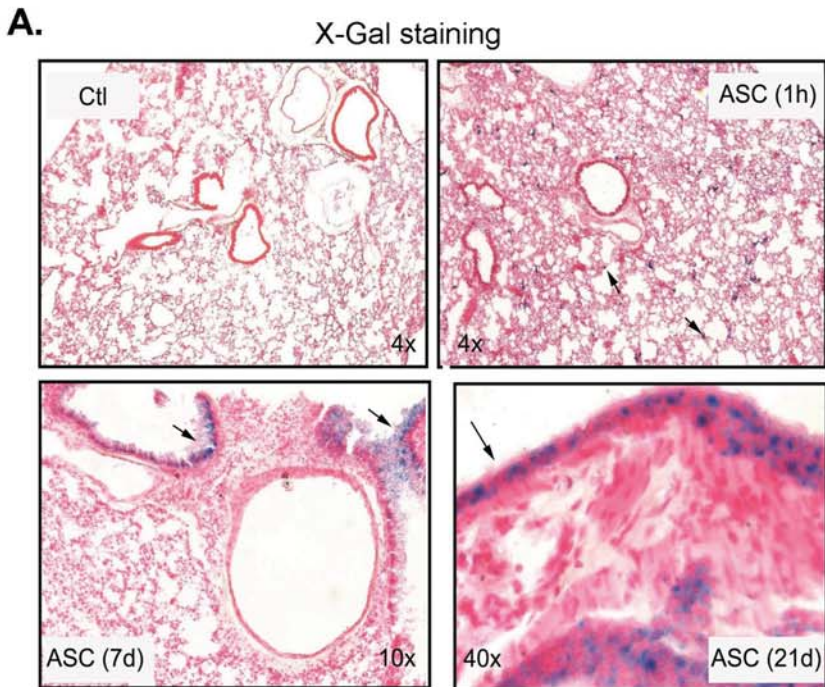


Figure 2

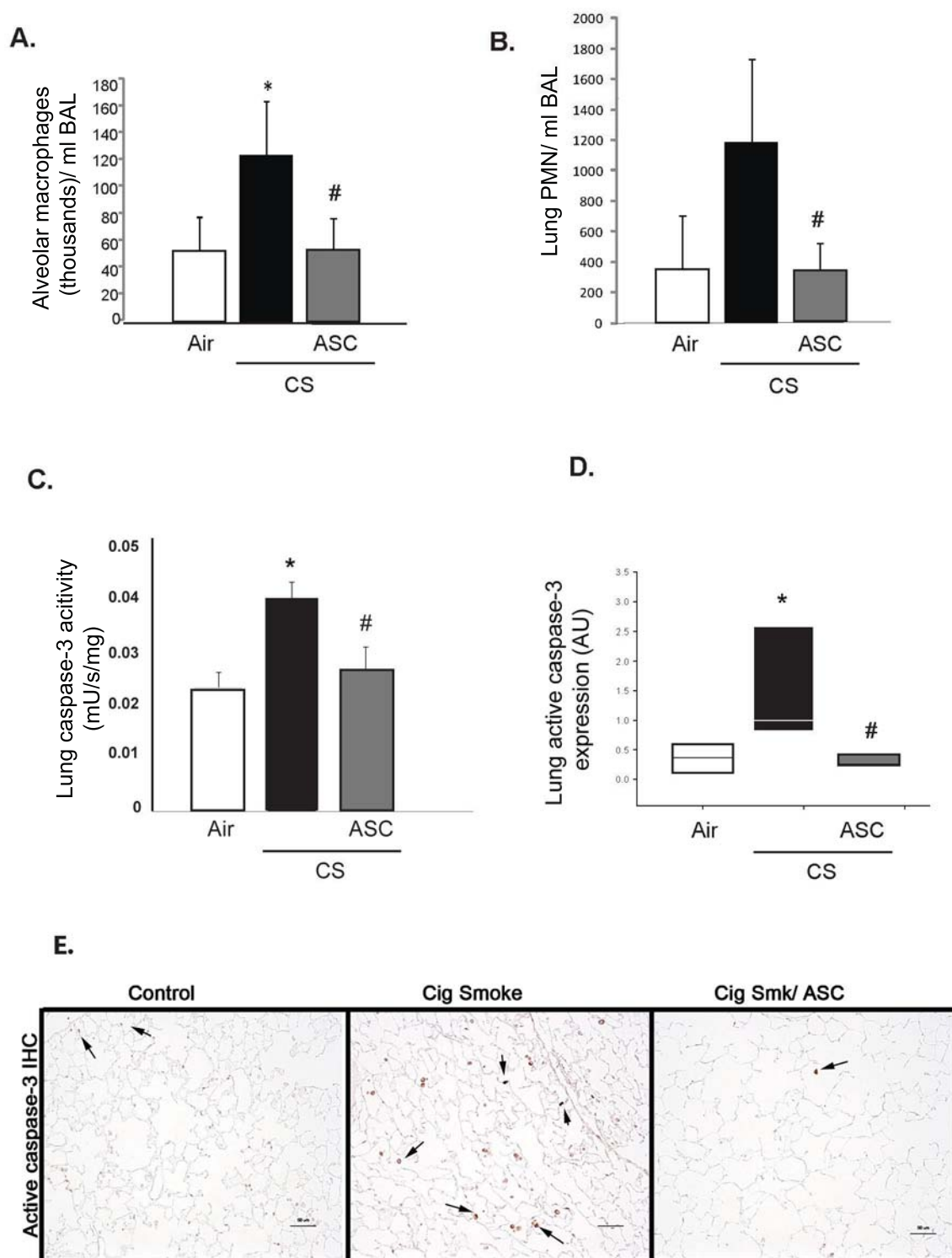


Figure 3

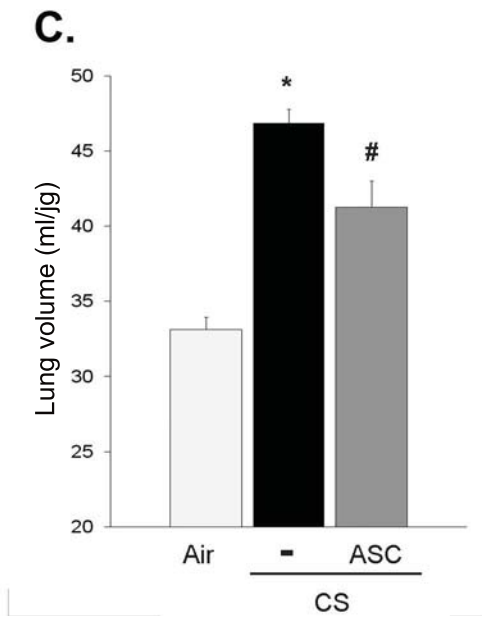
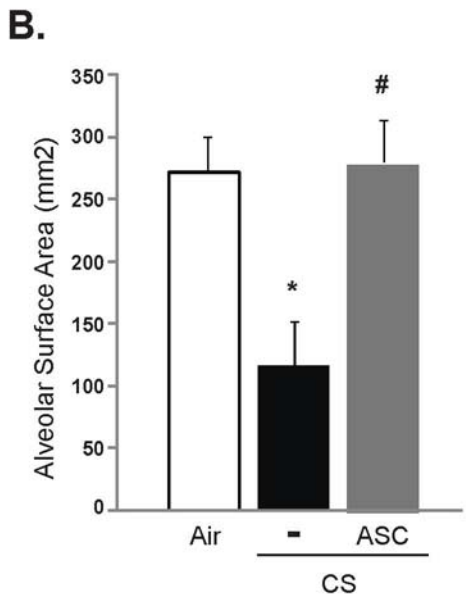
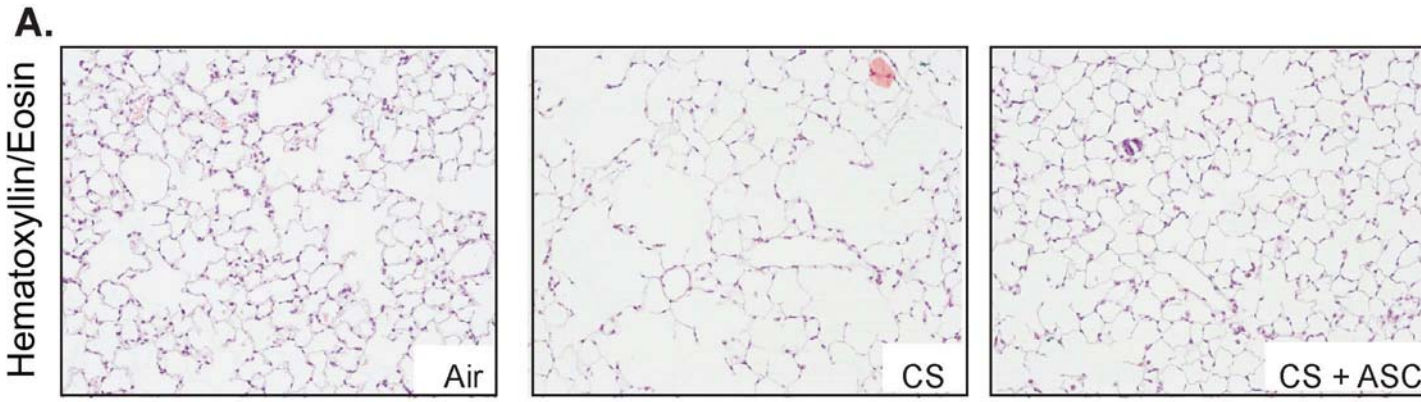


Figure 4

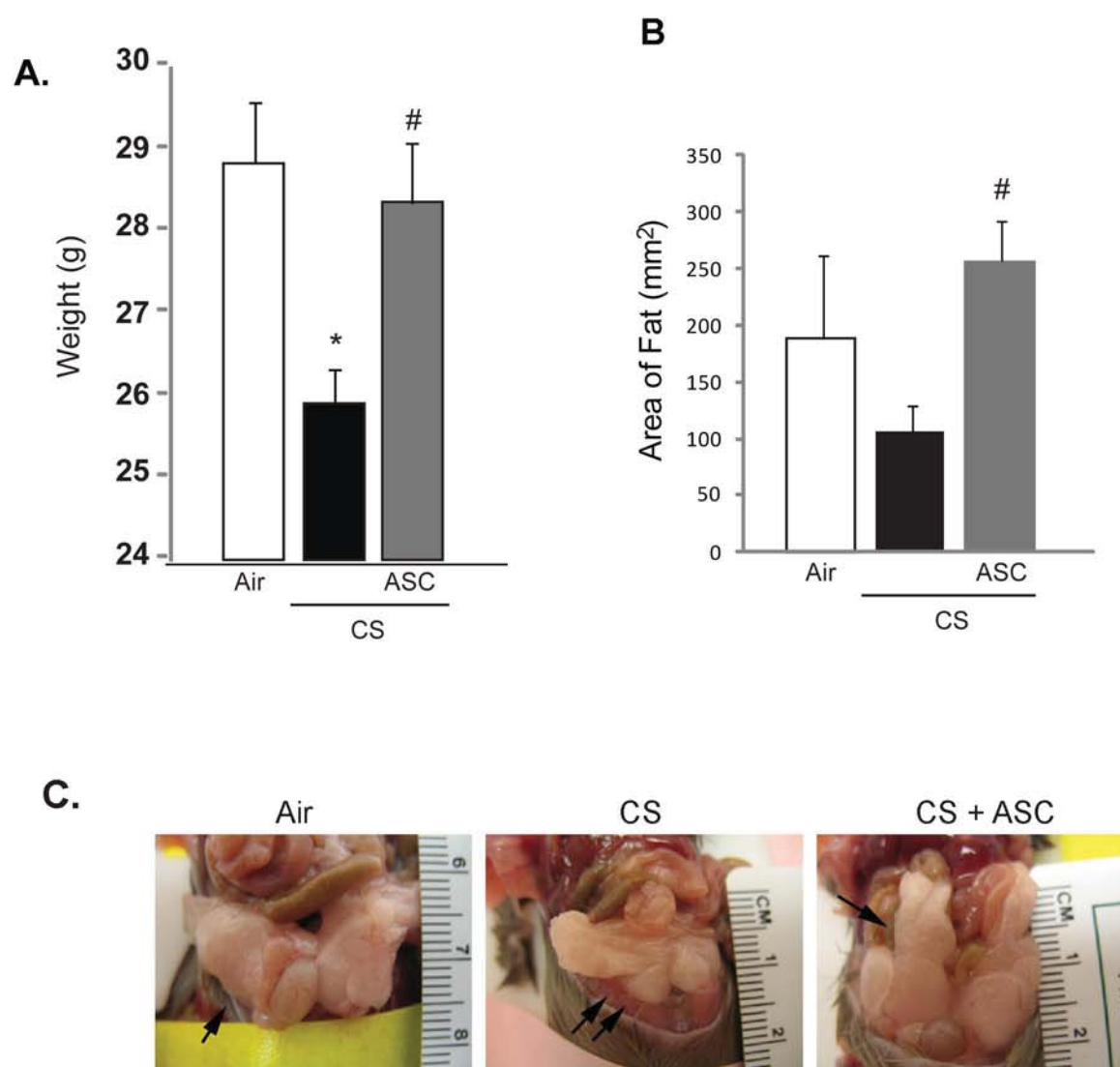


Figure 5

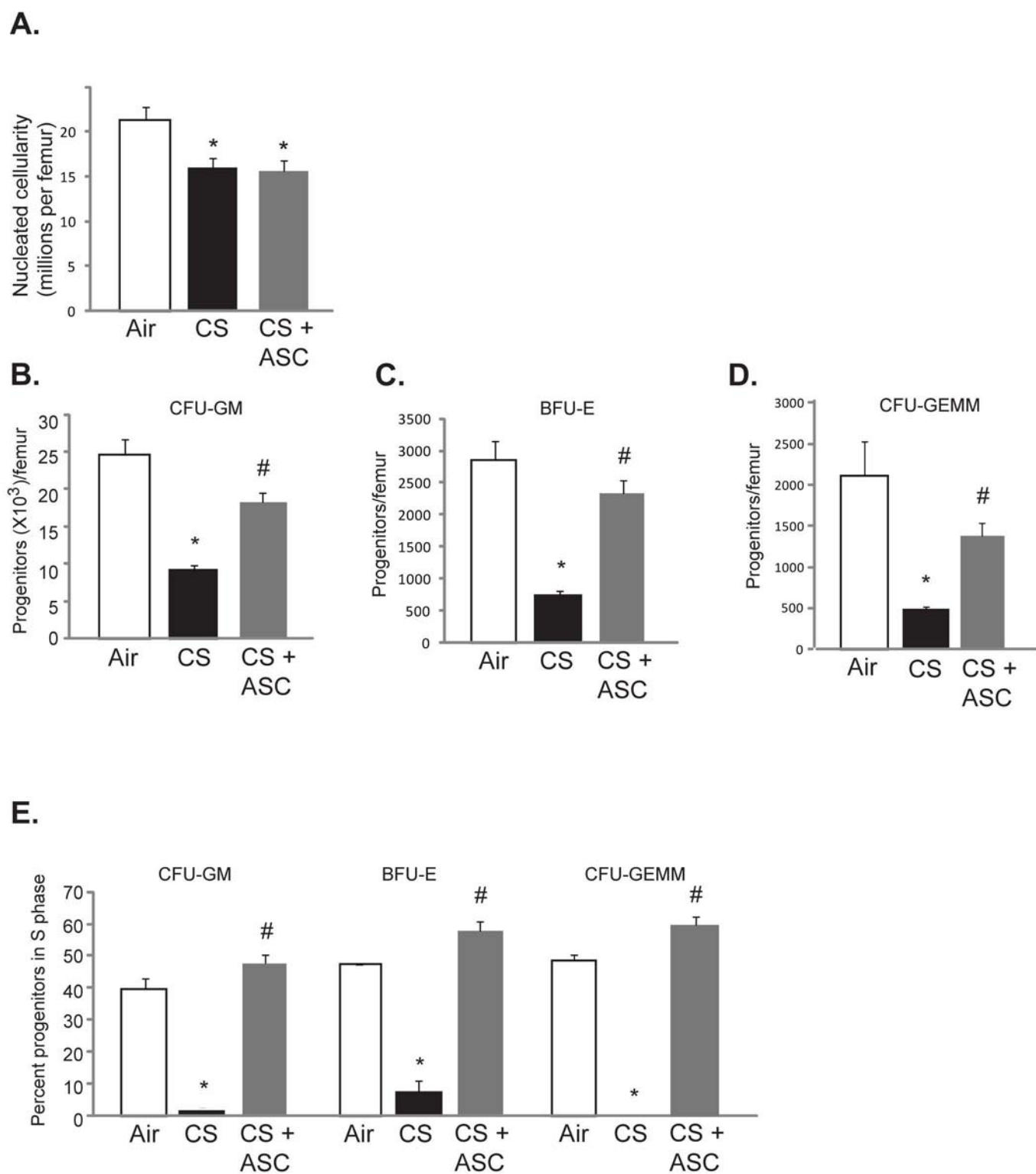
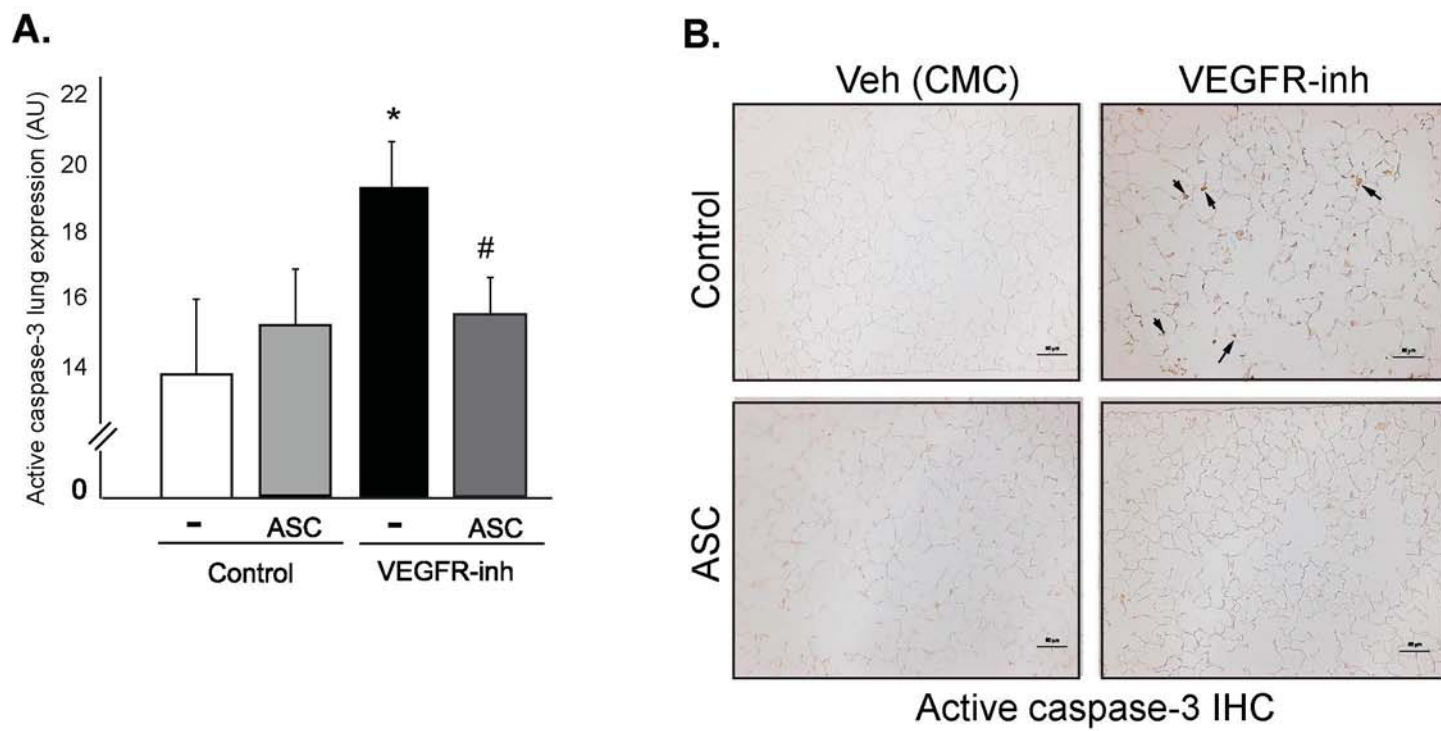
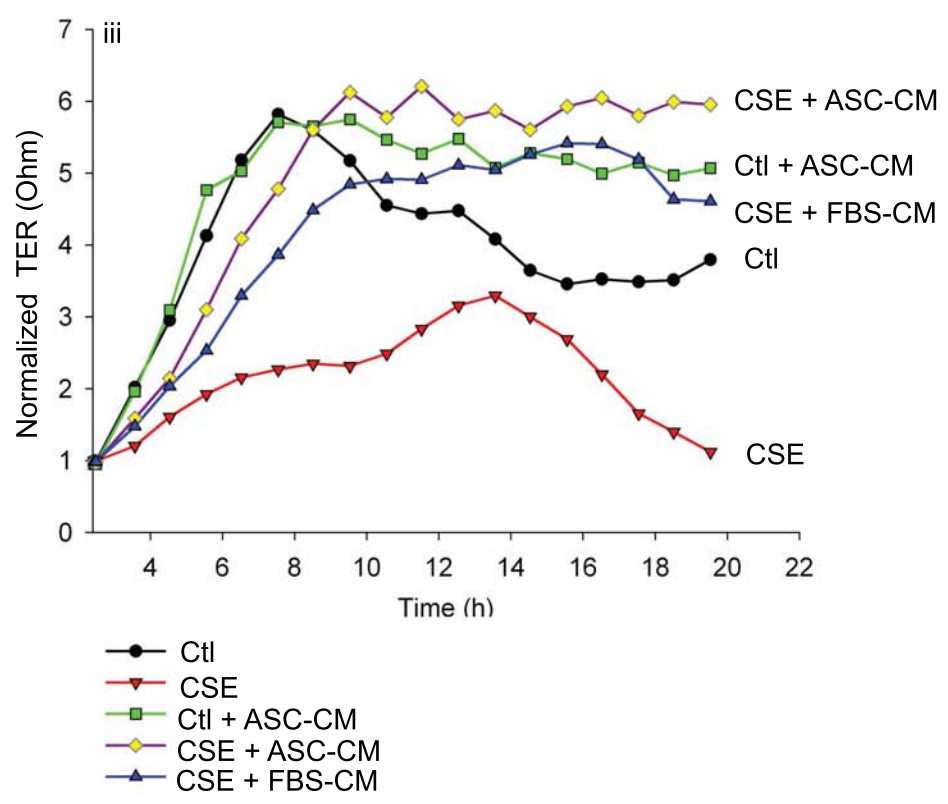
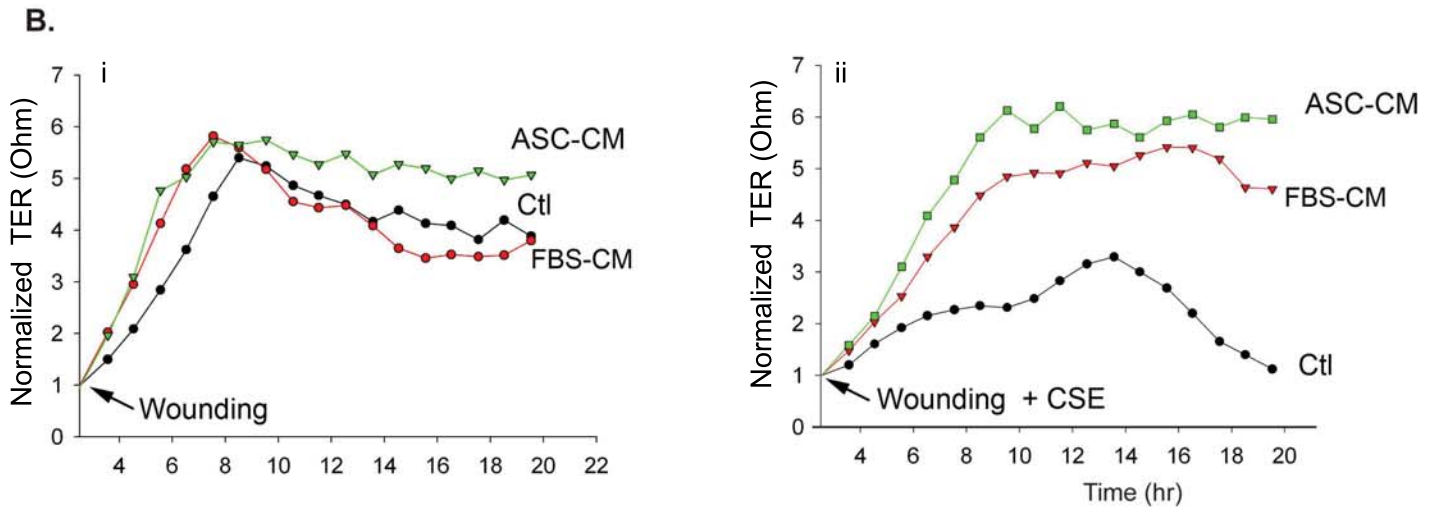
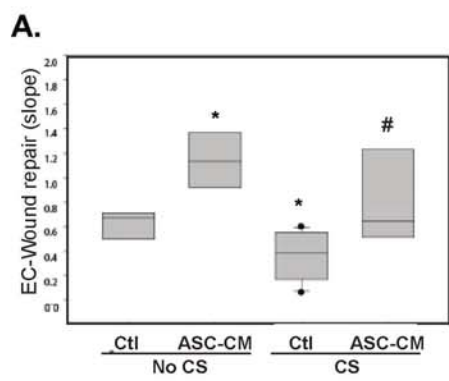


Figure 6





Online Data Supplement

**ADIPOSE STEM CELL TREATMENT IN MICE ATTENUATES LUNG AND
SYSTEMIC INJURY INDUCED BY CIGARETTE SMOKING**

Kelly Schweitzer, Brian H. Johnstone, Jana Garrison, Natalia Rush, Scott Cooper, Dmitry O. Traktuev, Dongni Feng, Jeremy J. Adamowicz, Mary Van Demark, Amanda J. Fisher, Krzysztof Kamocki, Mary Beth Brown, Robert G. Presson, Jr., Hal E. Broxmeyer, Keith L. March, and Irina Petrache

Figure E1. ASCs home to mouse lungs following systemic injection. **A.** ASC were intravenously delivered into ApoE mice and assessed for B-galactosidase expression at 1hr in fresh lungs. Note the vascular distribution of the blue-stained ASC (arrows). **B.** Biochemical quantification of lung ASC by immunoblotting with a specific GFP antibody of lung lysates obtained at day 3 following the intravenous injection of GFP-labeled ASC into NS2 mice that were also treated with a VEGFR inhibitor SU5416 (20mg/kg) or its vehicle (-). Vinculin was used as a loading control. **C-D.** Localization of GFP-expressing murine ASC (brown, arrow) on lung sections following fixation and immune staining with GFP antibody (C, D) and counterstaining with hematoxylin (C). Lungs of DBA/2J mice were harvested 7 days following ASC administration (3×10^5). Note (arrows) the presence of ASC intercalated among the bronchial epithelial layer (C) and in the lung parenchyma (D). Barsize 100 μm . **E.** Flow cytometry panels showing detection of events consistent with Di-I-labeled murine ASC in lung homogenates of DBA2 mice, 21 days following ASC intravenous injection, compared to control littermate mice, which did not receive ASC. Note in red, fluorescent cells comprising approximately 4% of total cell population, in the ASC-injected mice.

Figure E2. ASC treatment modulates the CS-induced activation of MAPK and AKT signaling pathways. **A-C.** Levels of p38 MAPK, JNK1, and Akt activation measured by densitometry of phosphorylated proteins relative to total levels of respective proteins detected by immunoblotting of total lung homogenates with specific antibodies. The lungs from DBA/2J mice were harvested following 4 months of air or CS exposure. A third group was treated with ASC (3×10^5 cells per injection, injected intravenously

every other week), during the month 3 and 4 of CS exposure (mean + SEM; n=4-6 lung samples from individual mice; *p<0.05 versus air control; #p<0.05 versus CS; ANOVA).

Figure E3. ASC attenuate the weight loss caused by CS. Representative photographs of mice following 4 months of air or CS exposure and of CS-exposed mice treated with ASC during the last 2 months of exposure. Note the smaller size (girth) of CS-exposed mice and the similar size of ASC-treated CS-exposed mice compared to control mice.

Figure E1

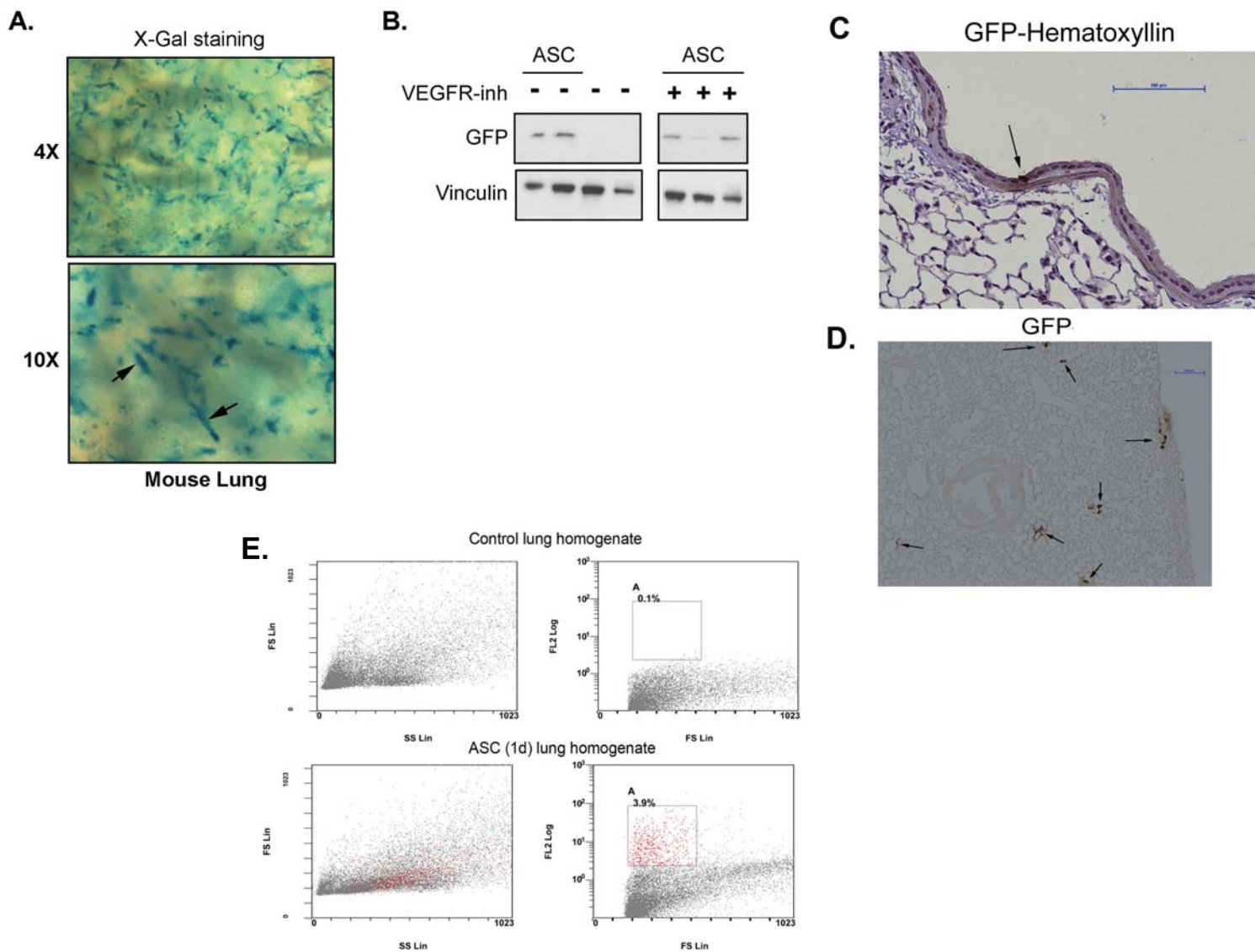


Figure E2

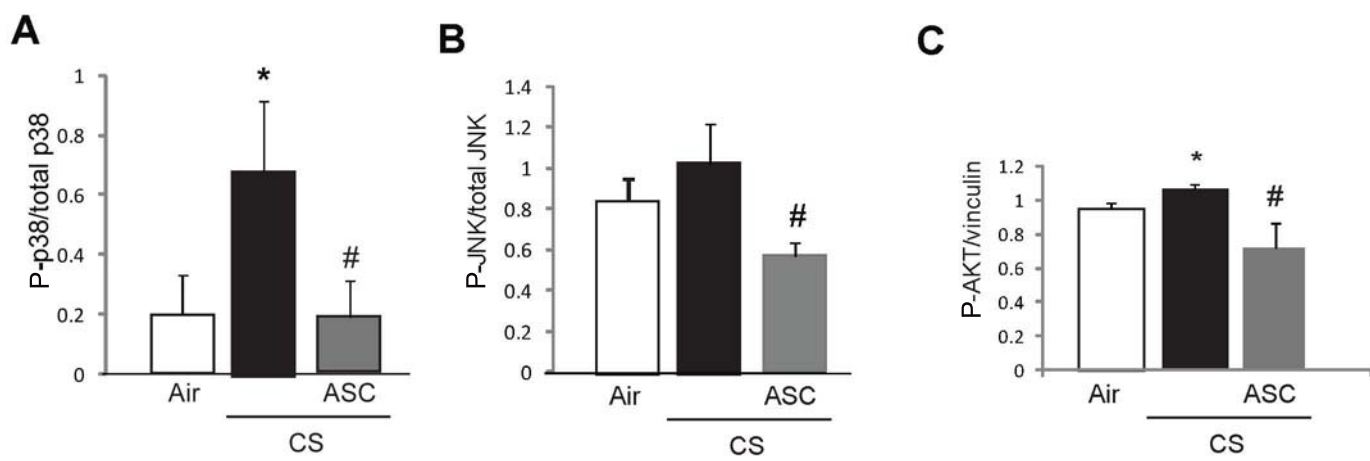


Figure E3

